Developmental and Comparative Immunology 34 (2010) 76–83

Contents lists available at ScienceDirect

Developmental and Comparative Immunology

journal homepage: www.elsevier.com/locate/dci

First identification and functional analysis of a histidine triad nucleotide binding protein in an invertebrate species *Haliotis diversicolor supertexta*

Liuji Wu [a], Xinzhong Wu [a,*], Hongkuan Deng [b], Yanqing Huang [a]

[a] *Laboratory of Marine Life Science and Technology, College of Animal Sciences, Zhejiang University, 268 Kaixuan Road, Hangzhou 310029, PR China*
[b] *Key Laboratory of Zoonoses, Ministry of Education, Institute of Zoonoses, Jilin University, 5333 Xian Road, Changchun 130062, PR China*

ARTICLE INFO

Article history:
Received 11 March 2009
Received in revised form 21 August 2009
Accepted 21 August 2009
Available online 4 September 2009

Keywords:
Pro-apoptotic factor
HINT
Haliotis diversicolor supertexta
Immune response
Immunostainings
p53

ABSTRACT

Histidine triad nucleotide binding protein (HINT) represents the most ancient and widespread branches in the histidine triad superfamily. HINT plays an important role in many biological processes especially in cell biology, and it has been found in a wide variety of species. However, the functional attributes of HINT homologues in invertebrates have not yet been reported. Here we identified a HINT homologue in abalone, which we named ab-HINT. The ab-HINT shows significant structural and functional similarities to mammalian HINT. RT-PCR and western blot analysis show that ab-HINT is ubiquitously expressed in abalone tissues and highly expressed in hemocyte and gills. In addition, significant up-regulation of ab-HINT was observed after LPS or Poly I:C challenge. Immunostainings suggest that ab-HINT is expressed predominantly in epithelial cells and mainly localized in the cytoplasmic compartment. Studies of the effect on cell apoptosis indicate that ab-HINT can trigger hemocytes apoptosis and p53 is involved in this process. These results conclude that ab-HINT is involved in the immune response of abalone and may be a potential pro-apoptotic factor. To the best of our knowledge, this is the first identification and characterization of a HINT homologue in invertebrates.

1. Introduction

Histidine triad nucleotide binding protein (HINT, also designated HINT1) was originally isolated through biochemical purification and sequencing from bovine brain and described as an inhibitor of protein kinase C [1]. However, subsequent studies have cast doubt on this function, and it was named PKCI (protein kinase C-interacting protein) because it interacts with protein kinase[(pTJ9s)1361414.y4b(s)816.3(5(d990.4This)-280ein-1s3159TD[(in)ataxia-)(e)bnote446.l600.4scn.29 classified in five branches [5]. The HINT branch is the most conserved member of the HIT superfamily, and HINT homologues are present in a wide variety of organisms including metazoan, plant, fungus, and bacterial kingdom [6]. The HINT proteins have more than 90% identity of overall amino-acid sequence in known mammalian orthologues. The *Mycoplasma genitalium* genome, which is known to be the smallest genome of any free-living organisms, shares over 30% identity with human HINT [7]. Strongly conservative sequence suggests that these proteins play a fundamental role in cell biology. HINT has been shown to be an efficient aminoacyl-adenylate and acyl-adenylate hydrolase [8,9]. Meanwhile, it was reported that HINT can regulate the activity of the microphthalmia transcription factor and, probably, other transcription factors [10]. In addition, the recent studies have suggested that mammalian HINT is involved in the modulation of apoptosis in cancer cells and may be a potential tumor suppressor [11–14].

The second branch of the HIT superfamily is FHIT (fragile locus HIT protein), which is only found in eukaryotes with representative sequences in human and yeast. It was originally isolated by linkage analysis at the human chromosome locus 3p14.2 and was also reported as a tumor suppressor as well as HINT [15]. The third apraxia1 [16,17] and possesses phosphoramidase and Ap_4A (diadenosine tetraphosphate) hydrolase activity as well as DNA/RNA binding properties [18]. The fourth branch is the GalT (galactose-1-phosphate uridylyltransferase) branch which shares only a little of overall sequence similarity with HINT or FHIT branch members, but its three-dimensional structure is quite similar to that of HINT and FHIT branch members [3]. The last branch is scavenger mRNA decapping enzyme, DcpS/DCS-1, which is a 7-methyl-GpppG hydrolase [19]. Based on crystal structure analysis, HINT was suggested to be a common ancestor of the other four branches [3].

* Corresponding author. Tel.: +86 571 86971960.
E-mail address: wuxz@zju.edu.cn (X. Wu).

0145-305X/$ – see front matter © 2009 Elsevier Ltd. All rights reserved.
doi:10.1016/j.dci.2009.08.008

Despite the fact that HINT-related gene sequences have been reported in several species of invertebrates, those studies were just limited to the sequence analyses with genomic or proteomic approaches. Therefore, little is known regarding the biochemical and physiological functions, especially the immune-related functions of HINT in invertebrates. Abalone is one of the most important mollusc species for commercial production in the world. In recent years, the global industry of abalone has been gradually decreased because of diseases or environmental pollution [20]. However, the molecular mechanisms of immunity in invertebrates, including abalone, are far from being understood. The relationship between immunity and apoptosis is not clear [21]. To study the molecular mechanisms of immunity, we have identified two immune-related proteins in abalone *Haliotis diversicolor supertexta* [22,23]. In the present study, we discovered a HINT homologue from an abalone cDNA library which we named ab-HINT. After sequence analyses, identification of dimeric structure and enzymatic activity, we demonstrate that ab-HINT is structurally and functionally homologues to the mammalian HINT. Studies on the physiological functions of ab-HINT indicate that ab-HINT plays a role in abalone immune system and may trigger hemocytes apoptosis through up-regulating the expression of p53.

2. Materials and methods

2.1. Animals, tissue collection, and immune challenge

Healthy abalones (*H.diversicolor supertexta*), 3 years of age, were collected from an abalone farm in Xiamen (Fujian, China) and kept in artificial seawater with a cycling system at 23 °C [22]. Tissue collection and immune challenge were performed as we reported before [23]. A minimum of five individuals was used in each experimental condition. Abalones were challenged by injecting 50 μL *E.coli* lipopolysaccharide (LPS) or viral mimic Polyriboinosinic polyribocytidylic acid (Poly I:C) (1 μg/μL diluted in sterile 0.9% sodium chloride). In addition, abalones challenged with 50 μL autoclaved 0.9% sodium chloride were used as control.

2.2. Preparation and screening of abalone cDNA library

An abalone cDNA library has been constructed previously [23]. Screening of the abalone cDNA library was based on polymerase chain reaction (PCR) with the specific primers (Table 1). Positive plasmid clones were grown in liquid cultures and induced to a high copy number for direct sequencing.

2.3. Sequence analysis and phylogenetic construction

Sequence analysis was carried out by BLAST software. Deduced amino acid sequences were aligned using ClustalW software. A phylogenetic tree was constructed based on full length amino acid sequences using the neighbor-joining method and was drawn using MEGA version 3.1.

2.4. PCR analysis

Total RNAs from different tissues of healthy abalones or hemocytes of abalones challenged with 50 μL *E.coli* LPS (serotype 0.55:B5, purified by ion-exchange chromatography, Sigma; 1 μg/μL diluted in sterile 0.9% sodium chloride), viral mimic Poly I:C or equal volume of autoclaved 0.9% sodium chloride were isolated using TRIzol reagent (Invitrogen, USA). Semiquantitative RT-PCR was carried out as described previously [24] to examine the tissue distribution and the potential physiological function of ab-HINT. Specific primers of ab-HINT and β-actin are shown in Table 1.

2.5. Protein expression and purification

Based on the entire ab-HINT coding region sequence, specific PCR primers (shown in Table 1) were designed to amplify the mature protein. PCR products were digested with restriction enzymes (EcoRI, XhoI) and ligated to the PET-28 (a+) expression vector (Novagen, USA). After the recombinant plasmids were propagated in *E.coli* DH5a, they were transformed into *E.coli* BL21 (DE3) for protein expression. Then the recombinant fusion proteins were purified by affinity chromatography using the nickel-nitrilotriacetic acid agarose (Ni-NTA) resins (Qiagen, Germany) following the manufacturer's protocol. The purified recombinant protein was analyzed by 12% SDS-polyacrylamide gel electrophoresis at 25 mA for 2 h. The protein separation was visualized with Coomassie brilliant blue R-250 (Sigma, USA).

2.6. Identification of recombinant ab-HINT

Recombinant ab-HINT protein after purification was excised from a 12% SDS polyacrylamide gel, reduced with an excess of DTT, alkylated with iodoacetamide, and was treated with sequencing grade, modified trypsin (Promega, USA). The resulting peptides were extracted from the gel, desalted, and concentrated on a Magic C18 (Michrom BioResources, USA) column for Liquid Chromatography using a Michrom Paradigm MG4 system (Michrom BioResources, USA). The eluted peptide was used for electrospray ionization tandem mass spectrometry (MS) analyses on a LTQ-Orbitrap (Thermo Finnigan, USA). The scanning range of m/z was 300–2000 and the mass resolution R was 60,000.

2.7. Biological activity

The enzymatic activity of the ab-HINT was performed using high-performance liquid chromatography (HPLC) analysis equipped with a UV detector (Agilent 1100, USA). Adenosine-5′-monophosphoramidate (AMP-NH2, 500 μM) was used as a substrate and was incubated in the presence or absence of fusion protein (50 μg) in 250 mM HEPES, pH 5.5, and 5 mM $MgCl_2$ at 37 °C for 30 min in a total volume of 1 ml. The reaction was stopped by shot-freezing in liquid nitrogen [11]. After filtration on 0.22 μm Nylon Membrane filters (Millipore, USA), 20 μl of the reaction solution was injected in a reverse phase C-18 HPLC column, eluted in buffer (10 mM KH2PO4, 2 mM tetrabutylammoniumbromide, 3% acetonitrile, pH 6.0) with a running time of 15 min at a flow rate of 1 ml/min. The retention time and peak areas were monitored at 254 nm. Reaction products were identified by retention times obtained from standard AMP-NH_2 substances. Experiments were performed in triplicate and the data were represented as the mean ± SEM (n = 3) for Student's t

2.8. Dimeric structure

The dimeric structure of the ab-HINT fusion protein was performed on a Beckman-Optima XL-A analytical ultracentrifugation. Sedimentation velocity experiments were conducted at 20 °C, 120,000 × *g*, using an An-60 Ti rotor and 1.2 cm path-length cell. Data were collected at 280 nm and at a spacing of 0.003 cm with three averages in a continuous scan mode. Sedimentation coefficients were obtained with the software sedfit94. The values were reduced to water and 20 °C using standard procedures. The buffer density and viscosity were calculated by the software Sednterp. The ratio f/f_0 was calculated from the diffusion coefficient, which in turn is related to the spreading of the boundary, using the program Sedfit94. The Stokes radius (R_S) was calculated from the sedimentation coefficient by means of the Siegel and Monty equation, namely $S = M(1 - V_2\rho)/N_0(6\pi\eta R_S)$. The final result was exhibited by a figure performed by origin6 program.

2.9. Antibody

Anti-ab-HINT antibody was prepared as recently reported [25] with purified ab-HINT protein. In brief, purified proteins were homogenized in complete Freund's adjuvant (Sigma, USA). New Zealand White rabbits were immunized with purified proteins (2 mg for each rabbit), three times at 2-week intervals. Booster injections were given after another week with 1 mg purified proteins (diluted with incomplete Freund's adjuvant). Rabbit serum was collected 10 days after the last immunization. Other primary antibodies used were: anti-β-actin antibody, bs-0061R (Bios, China); anti-p53 antibody, ab16121 (Abcam, UK); anti-Bax antibody, sc-6236 and anti-Bcl-2 antibody, sc-783 (Santa Cruz Biotechnology Inc, USA). FITC-conjugated anti-rabbit secondary antibody (sc-3839, Santa Cruz Biotechnology Inc. USA) was used for immunofluorescence.

2.10. Immunohistochemistry and immunofluorescence

Immunohistochemistry was performed as previously reported [23] using the prepared antibody. Indirect immunofluorescence was detected using the antibody and the previously reported [26] method. Immunofluorescent staining was visualized by fluorescence microscopy (Olympus Ax70, Hamburg, Germany).

2.11. Preparation and treatment of hemocytes

Hemocytes culture was prepared as previously described [21]. Briefly, hemocytes were pooled from several individuals and collected to obtain 20 ml samples and adjusted to10^6 cell/ml by the addition of modified Hank's balanced salt solution (MHBSS). 1 ml of cell suspension (10^6 cells) was dispensed into 35 mm petri dishes together with 1 ml of MHBSS. Cells were allowed to attach for 20 min and carefully rinsed with MHBSS. Before incubation with 50 μl recombinant ab-HINT proteins (1 μg/μl), hemocytes were maintained at 15 °C in IMDM (Gibco), adjusted to ambient salinity (31 ppm), containing 5% heat inactivated horse serum, 5% heat inactivated fetal bovine serum, penicillin G (50 units/ml) and streptomycin (50 μg/ml).

2.12. Scanning electron microscopy and flow cytometry for apoptosis analysis

After incubation with ab-HINT protein (The group incubated with the dilution buffer of ab-HINT protein was used as control), the cultured hemocytes were collected and manipulated for scanning electron microscopy [21]. They were observed and photographed in SEM of Philips Model XL30 ESEM to examine the characteristic of apoptotic cells. In addition, flow cytometry was further used to detect the apoptotic cells by an Annexin V/PI apoptosis kit (MultiSciences Biotech, china). Briefly, cells (5×10^{-5}) were collected by centrifugation (500 × *g* for 15 min) and resuspended in Annexin-binding buffer, then labeled with Annexin V-FITC according to the manufacturer's instruction. PI was added to the samples immediately before flow cytometry measurement. FITC and PI-fluorescence were collected to distinguish among live, early, and late apoptotic or necrotic cells. The data were analyzed by FACSCalibur (Becton Dickinson, USA) with CellQuest Software (Becton Dickinson).

2.13. Western blot analysis

Proteins were crudely extracted from hemocytes and other abalone tissues. The concentrations of the proteins were measured by the Bradford's method [27]. 25 μg proteins were separated on 12% SDS/PAGE gels, respectively and then transferred onto a polyvinylidene difluoride (PVDF) membrane by an electrophoretic transfer system (Bio-Rad, USA). Membranes were blocked for 1 h at room temperature with 5% skim milk in PBST (PBS pH 7.4, containing 0.1% Tween-20) and probed with primary antibody at 4 °C overnight. Subsequently, membranes were incubated with HRP-conjugated anti-rabbit and anti-sheep IgG antibody (Sigma, USA) for 1 h at room temperature. Immunoreactivity was detected with HRP-DAB Detection Kit (Tiangen, China).

3. Results

3.1. Identification of a mammalian HINT homologue

A 616 bp full length cDNA sequence (GenBank accession no, EU071816) was obtained by screening an abalone cDNA library. The nucleotide and deduced amino acid sequences of the full length cDNA are shown in Fig. 1A. This cDNA has an ORF of 375 bp encoding 125 amino acid residues which displays a calculated molecular mass of 13.7 kDa and a theoretical isoelectric point (PI) of 5.5. The 5′ and 3′ untranslated regions (UTR) contain 63 and 178 bp, respectively. A single typical polyadenylation signal (AATAAA) was found between nucleotides 572–577 in the 3′ UTR. Alignment with human HINT (61% identity) and *Rattus norvegicus* HINT (62% identity) shows that the abalone protein has three conserved domains including the HIT motif, helical regions and β-strands, which are the characteristics of HINT proteins (Fig. 1B). Thus, it is suggested that we have discovered a mammalian HINT homologue in an invertebrate abalone, which we named ab-HINT. The construction of an unrooted phylogenetic tree shows that the ab-HINT clusters with a branch of *Caenorhabditis elegans* and *Marine gamma proteobacterium* (Fig. 1C).

3.2. Recombinant protein production and identification

The ab-HINT recombinant protein was expressed in *E. coli* BL21 and purified from culture supernatant. One single band with an apparent molecular mass of 17.5 kDa (Fig. 2A) was displayed by SDS/PAGE analysis. The protein was then further identified by LC-MS/MS analyses. Fifty-five peaks were unambiguously identified as tryptic fragments of the recombinant protein (data were not shown). The sequence coverage of the matched protein overlapped for 72% with the amino acid sequence deduced from recombinant ab-HINT protein (Fig. 2B).

3.3. Dimeric structure and biological activity of ab-HINT

It is known that, via X-ray structural analysis, mammalian HINT forms homodimer [28,29]. The present analysis of amino acid

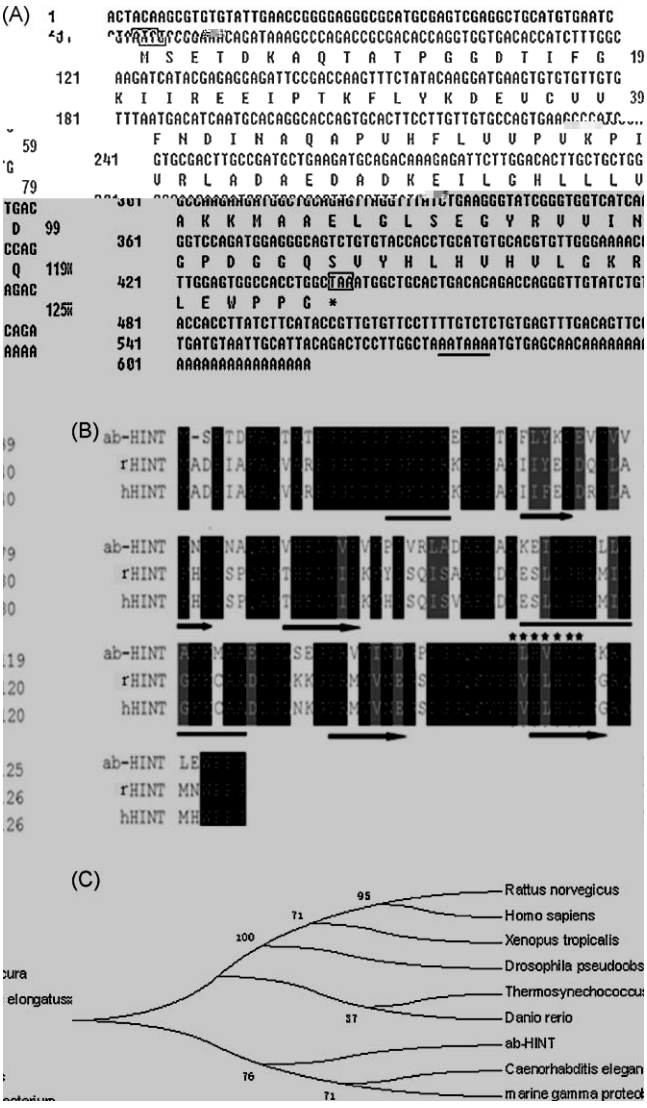

Fig. 1. (A) Nucleotide and deduced amino acid sequences of ab-HINT from abalone, *H. diversicolor supertexta*. The translation start (ATG) and stop (TAA) codon are indicated in boxes. The polyadenylation signal AATAAA is underlined. The nucleotides are numbered along the left margin and amino acids are numbered along the right margin. (B) Alignment of the ab-Hint amino acid sequences with that of human HINT and *Rattus norvegicus* HINT. Deduced amino-acid sequences of *Rattus norvegicus* (GenBank accession no, NP_071528), *Homo sapiens* (GenBank accession no, NP_005331) and *ab-HINT* (GenBank accession no, EU071816) were aligned by Clustal program, version 1.83. Conserved amino-acid were shaded and each shade represents a degree of conservation (black, 100%). HIT motif is denoted by asterisks over the aligned sequences, helical regions are underlined, β-strands are denoted by arrows. (C) Phylogenetic tree of representative hint superfamily proteins. The neighbor-joining distance tree was constructed based on the amino acid sequence alignments of hint superfamily proteins. Branch confidence levels (% based on 500 bootstrap replicates) reveal an evolutionarily ancient split into the ab-HINT branch and other HINT branches. GeneBank accession nos: *Xenopus tropicalis*, NP_001016165; *Drosophila pseudoobscura*, XP_001356002; *Rattus norvegicus*, NP_071528; *Homo sapiens*, NP_005331; Thermosynechococcus elongatus, NP_681787; *Caenorhabditis elegans*, NP_492056; *Danio rerio*, CAQ15082; *Marine gamma proteobacterium*, ZP_01627494 and *ab-HINT*, EU071816.

identity between ab-HINT and other mammalian HINT members has revealed two regions with strong sequence similarity, including helical regions and β-strands, which are crucial for homodimer formation of HINT proteins [7]. To confirm this hypothesis, we performed an experiment by analytical ultracentrifugation. The results show that the fusion protein ab-HINT has a molecular mass of 35 kDa (Fig. 3A), which is consistent with the

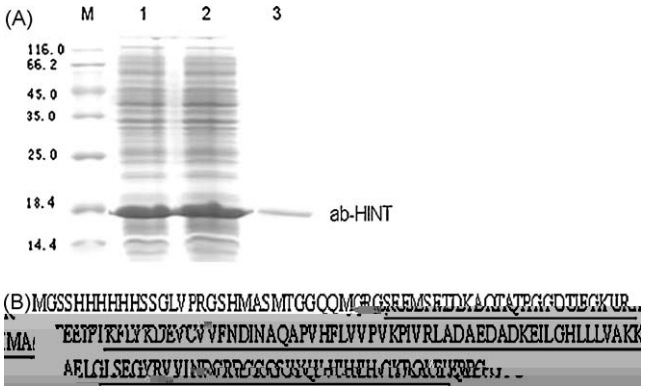

Fig. 2. (A) SDS-PAGE analysis of recombinant ab-HINT. Lane M: unstained protein standards (numbers are in kilodaltons); Lane 1: recombinant ab-HINT expression induced by 0.5 mM IPTG; lane 2: recombinant ab-HINT expression induced by 1 mM IPTG; lane 3: recombinant ab-HINT after purification. (B) Identification of the purified ab-HINT protein via sequencing by mass spectrometry. The peptide fragments of ab-HINT protein identified by analysis of mass spectrometry are underlined.

protein being a homodimer (the evaluated molecular mass of the monomer is 17.5 kDa).

We have found that ab-HINT contains the HIT domain which characterizes a superfamily of protein with nucleotide hydrolase or transferase activity [30]. We further investigated whether ab-HINT has activity characteristic as mammalian HINT using a HPLC method. The results showed that the concentration of AMP-NH_2 decreased drastically with the presence of ab-HINT (Fig. 3B).

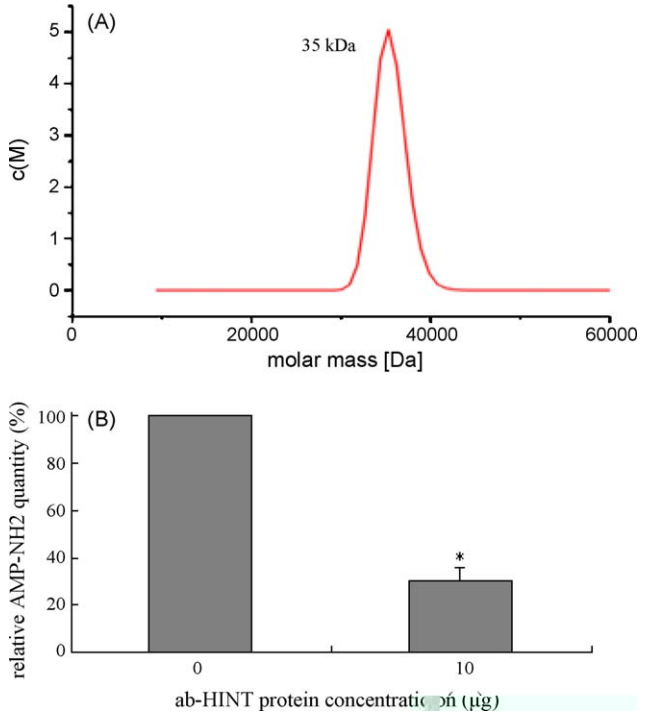

Fig. 3. (A) Predicted molecular mass of the ab-HINT fusion protein by analytical ultracentrifugation. It revealed a protein with apparent molecular mass of 35 kDa, which is consistent with the homodimer of ab-HINT fusion protein (the predicted molecular mass as a monomer is 17.5 kDa). (B) Adenosine-5′-monophosphoramidate (AMP-NH_2) hydrolase activity of recombinant ab-HINT protein. The concentration of AMP-NH_2 with the absence of recombinant HINT protein and the concentration of AMP-NH_2 after reaction with recombinant ab-HINT protein were determined by HPLC analysis. The data were normalized by the concentration with the absence of ab-HINT protein and analyzed by Student's *t*-test. Asterisk indicates statistically significant difference ($p < 0.01$).

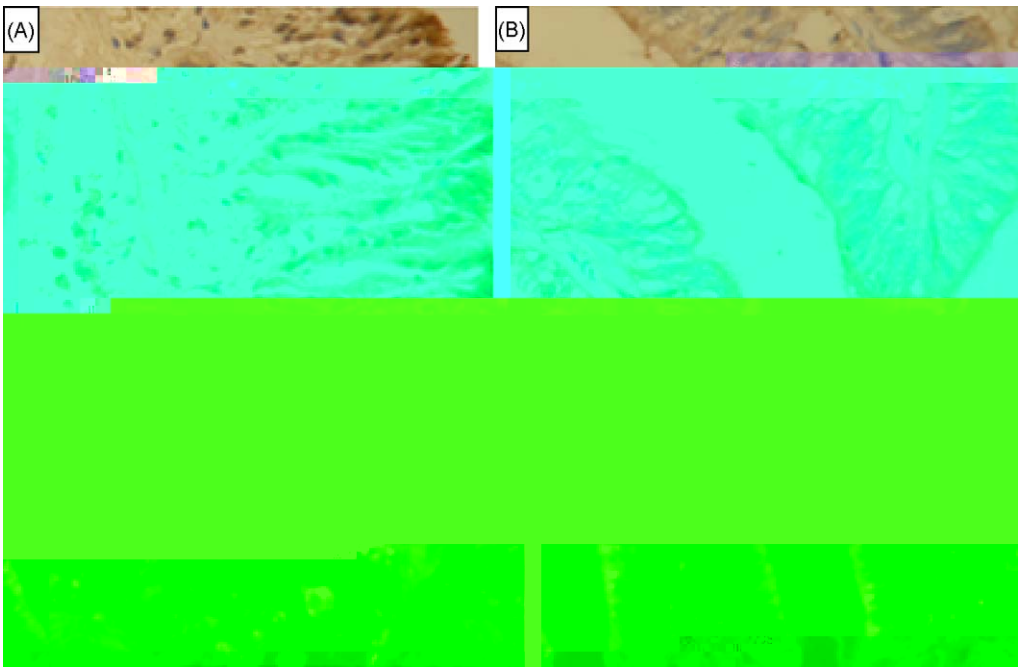

Fig. 4. Expression localization of ab-HINT in abalone mantle margin and gills. (A) Immunohistochemical staining of abalone mantle margin. (B) Immunohistochemical staining of abalone gills. (C) Immunofluorescent staining of abalone mantle margin tissue. (D) Immunofluorescent staining of abalone gills. Control samples showed no immunostaining (data not shown). Magnifications: A, 200; B–D 400.

3.4. Expression localization of ab-HINT

The specificity of the anti-ab-HINT antibody was analyzed by western blotting [23] and the results showed that the antibody was highly specific for ab-HINT (data not shown). To investigate the expression localization of ab-HINT in abalone tissues, we performed immunohistochemical staining using anti-ab-HINT antibody (Fig. 4A and B). In examined mantle margin and gills tissues, the ab-HINT was expressed predominantly in epithelial cells and mainly localized in the cytoplasmic compartment. These results were further confirmed by immunofluorescent staining (Fig. 4C and D).

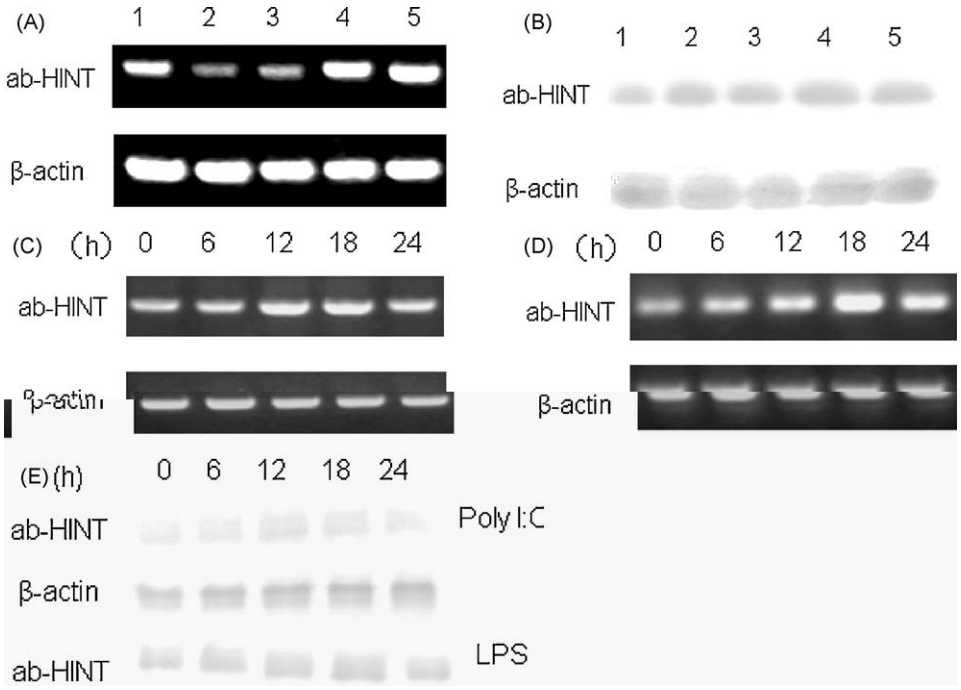

Fig. 5. (A) RT-PCR analysis of expression of ab-HINT in abalone tissues using the specific primers of ab-HINT. β-actin was used for endogenous control. (B) Expression of ab-HINT protein in abalone tissues was detected by western blot. β-actin was used for loading control. 1: mantle margin; 2: foot muscle; 3: digestive glands; 4: gills; 5: hemocyte. (C) RT-PCR analysis of expression levels of ab-HINT in hemocyte at 0, 6, 12, 18 and 24 h after LPS challenge. (D) RT-PCR analysis of expression levels of ab-HINT in hemocyte at 0, 6, 12, 18 and 24 h after Poly I:C challenge. β-actin was used for endogenous control. (E) Western blot analysis of expression levels of ab-HINT in hemocyte at 0, 6, 12, 18 and 24 h after Poly I:C and LPS challenge. β-actin was used for loading control.

3.5. Expression analysis of ab-HINT

To further investigate the potential function of ab-HINT in vivo, tissues distribution of ab-HINT was studied by RT-PCR and western blot analysis (Fig. 5A and B). The results showed that the ab-HINT was ubiquitously expressed in abalone tissues including hemocyte, gills, digestive glands, foot muscle and mantle margin. Moreover, relatively higher amount of ab-HINT was observed in abalone hemocyte and gills at the transcriptional level (Fig. 5A) as well as posttranscriptional level (Fig. 5B).

To test the hypothesis that ab-HINT is involved in the immune responses, RT-PCR was also used to analyze the expression level of ab-HINT in hemocyte after LPS and Poly I:C challenge, respectively. We observed that the expression levels of ab-HINT increased quickly after LPS and Poly I:C challenge and reached their peak levels at 12 and18 h, respectively (Fig. 5C and D). In addition, western blot analysis was used to examine the expression change of ab-HINT. The results showed that the posttranscriptional level of ab-HINT was also increased at 12 and 18 h after LPS and Poly I:C challenge (Fig. 5E). Meanwhile, no remarkable changes were revealed in control group at transcription level and post-transcription level (data not shown).

3.6. Ab-HINT induces abalone hemocytes apoptosis

To determine the physiological function of ab-HINT in hemocytes, scanning electron micrography, flow cytometry and western blotting were used for apoptosis analysis. Scanning electron micrography (Fig. 6A) showed that 24 h exposure to 50 μg of ab-HINT recombinant protein caused phenotypical changes in hemocytes. These changes included plasma membrane changes and the formation of blebs, which are characteristic of hemocytes undergoing apoptosis. The results from flow cytometry showed that the percentage of apoptotic hemocytes increased over time and reached 34% after 24 h of exposure to 50 μg ab-HINT fusion protein (Fig. 6B). Results of the comparison between control and experimental group showed that there were significant differences at 12 and 24 h after incubation. Meanwhile, there is no remarkable change in control group.

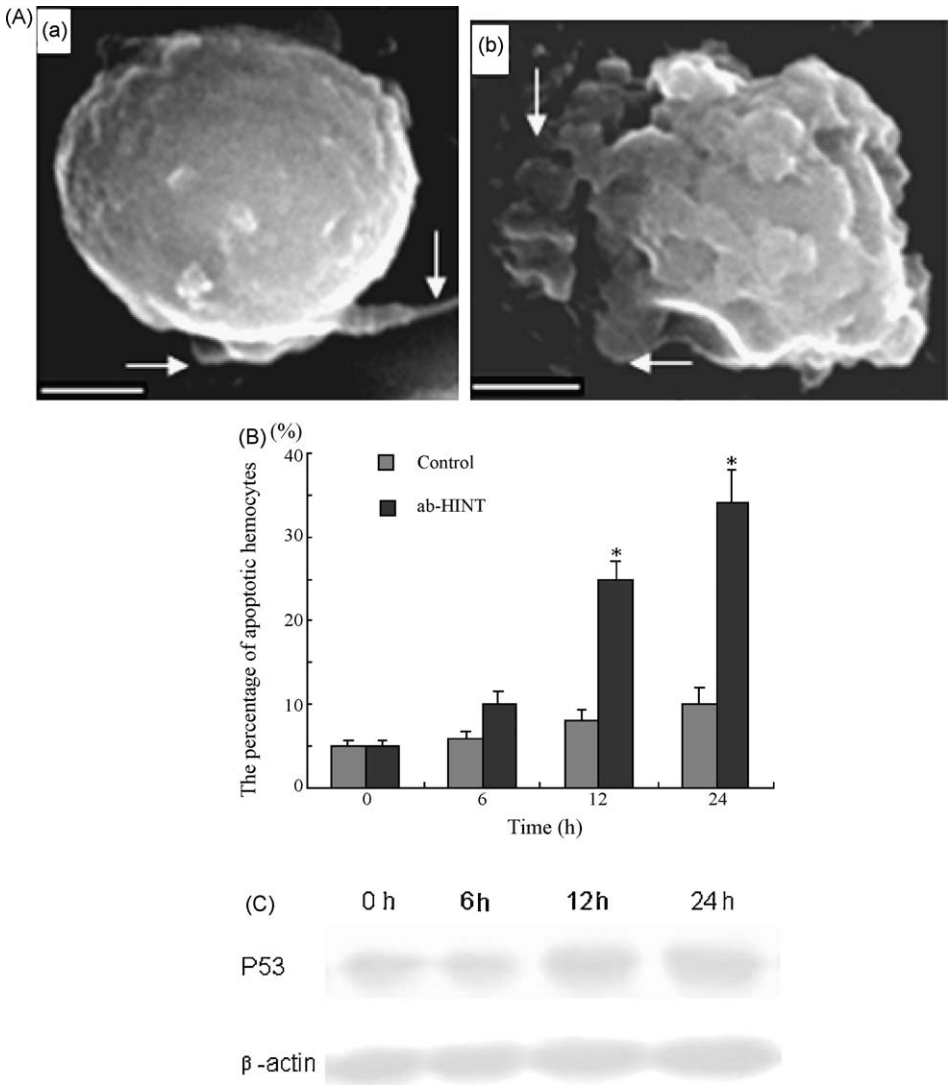

Fig. 6. (A) Scanning electron micrograph. (a) Control hemocyte. The cell tends to spread on the substrate and deploys several pseudopods (arrows). (b) Hemocyte incubation with 50 μg of ab-HINT fusion protein for 24 h. The cell exhibits visible membrane blebbing (arrows). Scale bars = 1 μm. (B) Time-dependent effect of ab-HINT on hemocytes apoptosis. The percentage of apoptotic hemocytes were analyzed by the Student's *t*-test method. Experiments were performed in triplicate and the data were represented as the mean ± SEM ($n = 3$). Differences were considered statistically significant when p values were less than 0.01. (C) Ab-HINT protein up-regulates expression of p53 in abalone hemocytes. The expression of p53 in hemocytes was analyzed with a polyclonal anti-p53 antibody by western blot after incubation with 50 μg of ab-HINT protein for 0, 6, 12, 24 h. β-actin was used for loading control.

[12] Wang L, Zhang Y, Li H, Xu Z, Santella RM, Weinstein IB. Hint1 inhibits growth and activator protein-1 activity in human colon cancer cells. Cancer Res 2007;67(10):4700–8.
[13] Li H, Zhang Y, Su T, Santella RM, Weinstein IB. Hint1 is a haplo-insufficient tumor suppressor in mice. Oncogene 2006;25(5):713–21.
[14] Su T, Suzui M, Wang L, Lin CS, Xing WQ, Weinstein IB. Deletion of histidine triad nucleotide-binding protein 1/PKC-interacting protein in mice enhances cell growth and carcinogenesis. Proc Natl Acad Sci USA 2003;100(13):7824–9.
[15] Ohta M, Inoue H, Cotticelli MG, Kastury K, Baffa R, Palazzo J, et al. The FHIT gene, spanning the chromosome 3p14.2 fragile site and renal carcinoma-associated *t*(3;8) breakpoint, is abnormal in digestive tract cancers. Cell 1996;84(4):587–97.
[16] Moreira MC, Barbot C, Tachi N, Kozuka N, Uchida E, Gibson T, et al. The gene mutated in ataxia-ocular apraxia 1 encodes the new HIT/Zn-finger protein aprataxin. Nat Genet 2001;29(2):189–93.
[17] Date H, Onodera O, Tanaka H, Iwabuchi K, Uekawa K, Igarashi S, et al. Early-onset ataxia with ocular motor apraxia and hypoalbuminemia is caused by mutations in a new HIT superfamily gene. Nat Genet 2001;29(2):184–8.
[18] Kijas AW, Harris JL, Harris JM, Lavin MF. Aprataxin forms a discrete branch in the HIT (histidine triad) superfamily of proteins with both DNA/RNA binding and nucleotide hydrolase activities. J Biol Chem 2006;281(20):13939–48.
[19] Liu H, Rodgers ND, Jiao X, Kiledjian M. The scavenger mRNA decapping enzyme DcpS is a member of the HIT family of pyrophosphatases. EMBO J 2002;21(17):4699–708.
[20] Gardner GR, Harshbarger JC, Lake JL, Sawyer TK, Price KL, Stephenson MD, et al. Association of prokaryotes with symptomatic appearance of withering syndrome in black abalone *Haliotis cracherodii*. J Invertebr–Path 1995;66(2):111–20.
[21] Lacoste A, Cueff A, Poulet SA. P35-sensitive caspases, MAP kinases and Rho modulate beta-adrenergic induction of apoptosis in mollusc immune cells. J Cell Sci 2002;115:761–8.
[22] Jiang Y, Wu X. Characterization of a Rel\NF-kappaB homologue in a gastropod abalone, *Haliotis diversicolor supertexta*. Dev Comp Immunol 2007;31(2):121–31.
[23] Wu LJ, Wu XZ, Zhu BJ, Cao XH. Identification and characterization of a novel cytidine deaminase in a gastropod abalone *Haliotis diversicolor supertexta*. Dev Comp Immunol 2009;33(5):709–17.
[24] Law FB, Chen YW, Wong KY, Ying J, Tao Q, Langford C, et al. Identification of a novel tumor transforming gene GAEC1 at 7q22 which encodes a nuclear protein and is frequently amplified and overexpressed in esophageal squamous cell carcinoma. Oncogene 2007;26(40):5877–88.
[25] Zhu B, Wu X. Identification of outer membrane protein ompR from rickettsia-like organism and induction of immune response in *Crassostrea ariakensis*. Mol Immunol 2008;45(11):3198–204.
[26] Martin PM, Dun Y, Mysona B, Ananth S, Roon P, Smith SB, et al. Expression of the sodium-coupled monocarboxylate transporters SMCT1 (SLC5A8) and SMCT2 (SLC5A12) in retina. Invest Ophthalmol Vis Sci 2007;48(7):3356–63.
[27] Bradford MM. A rapid and sensitive method for the quantitation of microgram quantities of protein utilizing the principle of protein-dye binding. Anal Biochem 1976;72:248–54.
[28] Lima CD, Klein MG, Hendrickson WA. Structure-based analysis of catalysis and substrate definition in the HIT protein family. Science 1997;278(5336):286–90.
[29] Krakowiak A, Pace HC, Blackburn GM, Adams M, Mekhalfia A, Kaczmarek R, et al. Biochemical, crystallographic, and mutagenic characterization of hint, the AMP-lysine hydrolase, with novel substrates and inhibitors. J Biol Chem 2004;279(18):18711–6.
[30] Brenner C. Hint, Fhit, and GalT: function, structure, evolution, and mechanism of three branches of the histidine triad superfamily of nucleotide hydrolases and transferases. Biochemistry 2002;41(29):9003–14.
[31] Swingley WD, Chen M, Cheung PC, Conrad AL, Dejesa LC, Hao J, et al. Niche adaptation and genome expansion in the chlorophyll d-producing cyanobacterium *Acaryochloris marina*. Proc Natl Acad Sci USA 2008;105(6):2005–10.
[32] Schneiker S, Martins dos Santos VA, Bartels D, Bekel T, Brecht M, Buhrmester J, et al. Genome sequence of the ubiquitous hydrocarbon-degrading marine bacterium *Alcanivorax borkumensis*. Nat Biotechnol 2006;24(8):997–1004.
[33] Liu F, Lu J, Hu W, Wang SY, Cui SJ, Chi M, et al. New perspectives on host-parasite interplay by comparative transcriptomic and proteomic analyses of *Schistosoma japonicum*. PLoS Pathog 2006;2(4):e29.
[34] Brzoska PM, Chen H, Levin NA, Kuo WL, Collins C, Fu KK, et al. Cloning, mapping, and in vivo localization of a human member of the PKCI-1 protein family (PRKCNH1). Genomics 1996;36(1):151–6.
[35] Bachere E, Gueguen Y, Gonzalez M, de Lorgeril J, Garnier J, Romestand B. Insights into the anti-microbial defense of marine invertebrates: the penaeid shrimps and the oyster *Crassostrea gigas*. Immunol Rev 2004;198:149–68.
[36] Canesi L, Betti M, Ciacci C, Scarpato A, Citterio B, Pruzzo C, et al. Signaling pathways involved in the physiological response of mussel hemocytes to bacterial challenge: the role of stress-activated p38 MAP kinases. Dev Comp Immunol 2002;26(4):325–34.
[37] Raff MC. Social controls on cell survival and cell death. Nature 1992;356(6368):397–400.
[38] Yu J, Zhang L. No PUMA, no death: implications for p53-dependent apoptosis. Cancer Cell 2003;4(4):248–9.
[39] Yu J, Zhang L. The transcriptional targets of p53 in apoptosis control. Biochem Biophys Res Commun 2005;331(3):851–8.
[40] Terahara K, Takahashi KG, Mori K. Apoptosis by RGD-containing peptides observed in hemocytes of the Pacific oyster, *Crassostrea gigas*. Dev Comp Immunol 2003;27(6-7):521–8.